BIOCHEMISTRY
including biophysical chemistry & molecular biology

Article

pubs.acs.org/biochemistry

The Helix Located between the Two Domains of a Mip-like Peptidyl-Prolyl *cis*−*trans* Isomerase Is Crucial for Its Structure, Stability, and Protein Folding Ability

Biswanath Jana and Subrata Sau*

Department of Biochemistry, Bose Institute, P-1/12, CIT Scheme VII M, Kolkata 700054, West Bengal, India

Supporting Information

ABSTRACT: FKBP22, a PPIase (peptidyl-prolyl *cis*−*trans* isomerase) produced by *Escherichia coli*, binds FK506 and rapamycin (both immunosuppressive drugs), shares significant homology with the Mip-like virulence factors, and has been thought to carry a long α-helix (namely α3) between its two domains. To understand whether the length of helix α3 plays any role in the structure, function, and stability of FKBP22-like proteins, we studied a recombinant *E. coli* FKBP22 (rFKBP22) and its four helix α3 mutant variants by various in vitro probes. Of the helix α3 mutants, two were deletion mutants (rFKBP22D5 and rFKBP22D30), whereas the two others were insertion mutants (rFKBP22I3 and rFKBP22I6). Our investigations revealed that the molecular dimensions, dimerization efficiencies, secondary structures, tertiary structures, stabilities, and protein folding abilities of all mutant proteins are different from those of rFKBP22. Conversely, the rapamycin binding affinities of the mutant proteins were affected very little. Urea-induced unfolding of each protein followed a two-state mechanism and was reversible in nature. Interestingly, rFKBP22D30 was the least stable, whereas rFKBP22I3 appeared to be the most stable of the five proteins. The data together suggest that length of helix α3 contributes significantly to the preservation of the structure, function, and stability of *E. coli* FKBP22.

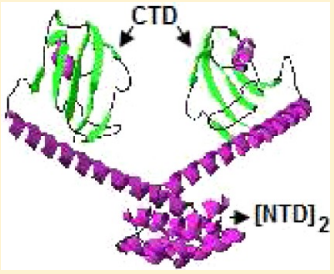

FKBP22, a protein produced by *Escherichia coli*,[1] possesses PPIase [peptidyl-prolyl *cis*−*trans* isomerase (EC 5.1.2.8)] activity,[2] exists as a homodimer in solution, and shares significant identity with various proteins such as *Legionella pneumophila* Mip,[3] *Chlamydia trachomatis* Mip,[4] *E. coli* FkpA,[5,6] *Trypanosmoa cruzi* Mip,[7] *Neisseria gonorrheae* Mip,[8] *Xanthomonas campestris* Mip,[9] *Salmonella typhimurium* FkpA,[10] and *Shewanella* sp. FKBP22.[11] Besides acting as the PPIase enzyme, Mip (macrophage infectivity potentiator) acts as a virulence factor in the pathogenic microorganisms. The catalytic activity in all the Mip and related proteins (including *E. coli* FKBP22) was inhibited by FK506 and rapamycin but not by other immunosuppressive drugs (such as cyclosporin A or juglone). A recent study suggested that an *E. coli* FKBP22 monomer harbors an N-terminal domain (NTD), a C-terminal domain (CTD), and a hinge region linking the two domains.[12] While a CTD with a truncated hinge region exhibited rapamycin binding ability, a recombinant NTD underwent dimerization in solution. Additional investigations revealed that urea- and GdnCl-induced equilibrium unfolding of a recombinant *E. coli* FKBP22 follows two-state and three-state mechanisms, respectively. Interestingly, the intermediate formed during the unfolding of recombinant FKBP22 with GdnCl was not a molten globule but was thought to be composed of the partially unfolded dimeric as well as various multimeric forms of this macromolecule.[12]

Both *L. pneumophila* Mip[13] and *E. coli* FkpA[14] proteins were shown to possess a V-shaped structure harboring two monomers. Each monomer is dumbbell-shaped with an N-terminal domain, a hinge region, and a C-terminal domain successively. The V-shaped dimeric structure that results from the interaction between the N-terminal domains of two monomers was suggested to be indispensable for the PPIase activity with a protein substrate.[15] The CTD harbors a peptide substrate binding site and the drug (FK506 and rapamycin) binding site. The "hinge" region, which presumably forms the arms of the V-shaped conformation and connects two domains, is mostly structured with an α-helix (designated α3) of ∼6.5 nm.[13] Such a long helix that lies between the two domains of the Mip-like proteins was not reported in other multidomain proteins. Two domains without the part of the helix α3 region appeared to be either nonfunctional or unstable.[15,16] Previously, the hinge region flanking the two domains of an *E. coli* FKBP22 monomer was suggested to harbor 32 amino acid residues.[12] Of the 32 residues, 26 residues seemed to form the N-terminal end of putative helix α3 in FKBP22. The remaining residues (∼12) of helix α3 located at its C-terminal end appeared to be buried within FKBP22.[12] Thus far, it is not known with certainty whether the length of helix α3 is essential for preserving the structure, function, and stability of the Mip-like proteins. Using four *E. coli* FKBP22 mutant proteins with the in-frame mutations in the helix α3-carrying region, here we report that the length of this region indeed plays a crucial role in

Received: June 1, 2012
Revised: September 14, 2012
Published: September 18, 2012

maintaining the structure, protein folding ability, and stability of *E. coli* FKBP22.

EXPERIMENTAL PROCEDURES

Materials. Urea, glutaraldehyde, acrylamide, bis-acrylamide, PMSF (phenylmethanesulfonyl fluoride), and IPTG (isopropyl β-D-1-thiogalactopyranoside) were purchased from Sigma, Merck, or SRL. Rapamycin was bought from BioVision. RNase T1 was bought from Fermentas. All other chemicals were of the highest purity available. The Ni-NTA resin and anti-His antibody were procured from Qiagen. The alkaline phosphatase-tagged goat anti-mouse antibody (IgG1-AP) was procured from Santa Cruz Biotechnology Inc. Restriction and modifying enzymes, the plasmid isolation kit, the QIAquick gel extraction kit, the polymerase chain reaction (PCR) kit, oligonucleotides, protein, and DNA markers were obtained from Qiagen, Genetix Biotech Asia Pvt Ltd., and Hysel India Pvt Ltd.

Bacterial Strains, Plasmids, and Oligonucleotides. All bacterial strains and plasmids used in the study are listed in Table S1 of the Supporting Information. *E. coli* DH5α, *E. coli* BL21(DE3), and their derivatives were routinely cultivated in Luria-Bertani broth supplemented with or without an appropriate antibiotic or IPTG.[17] Plasmid pET28a (Novagen) and *E. coli* strain BL21(DE3) were donated by the late P. Roy (Bose Institute). All oligonucleotides used in the study are listed in Table S2 of the Supporting Information.

Molecular Biological Methods. Plasmid DNA isolation, DNA estimation, digestion of DNA by restriction enzymes, modification of DNA fragments by modifying enzymes, plasmid DNA transformation of *E. coli*, PCR, purification of DNA fragments, agarose gel electrophoresis, sodium dodecyl sulfate–polyacrylamide gel electrophoresis (SDS–PAGE), staining of polyacrylamide gels, and Western blotting were performed by the standard methods[17,18] or according to the protocols provided by the respective manufacturers (Qiagen, Fermentas GmbH, and Bangalore Genei P. Ltd.). The total protein content was estimated by the Bradford assay using bovine serum albumin as the standard.[19] Sequences of all PCR-amplified DNA fragments were verified by DNA sequencing.

Construction of Plasmids and Strains. To express *E. coli* FKBP22 as a C-terminal end histidine-tagged variant (designated rFKBP22), plasmid p1289 (Table S1 of the Supporting Information) was constructed by cloning a DNA fragment (amplified by *Taq* DNA polymerase using p1280 DNA[12] as the template and primer pairs Nf and Cb) to pET28a. To express rFKBP22D5 (an rFKBP22 variant lacking five helix α3-forming amino acid residues), p1290 (Table S1 of the Supporting Information) was generated by cloning DNA fragment III to pET28a. Fragment III was made by ligating two *Sal*I-digested DNA fragments I and II, which were amplified by *Taq* DNA polymerase using p1280 DNA[12] and primer pairs Nf and 32B, and Cb and 32F, respectively. DNA fragment IV was made by ligating a *Sal*I-digested DNA fragment (amplified using *Taq* polymerase, p1280 DNA, and primers Nf and 7B) with a *Xho*I-digested DNA fragment (created using *Taq* polymerase, p1280 DNA, and primers 7F and Cb). Plasmid p1291 (Table S1 of the Supporting Information), generated by cloning fragment IV to pET28a, was used to express an rFKBP22 variant (designated rFKBP22D30) that is devoid of 30 helix α3-forming amino acid residues. To express protein rFKBP22I3 (an rFKBP22 variant whose putative α3 helix carries three additional amino acid residues), p1292 (Table S1 of the Supporting Information) was constructed by cloning DNA fragment VII to pET28a. Fragment VII was made by ligating *Sal*I-treated DNA fragments V (synthesized by *Taq* polymerase, p1280 DNA, and primers Nf and 40B) and VI (prepared by *Taq* polymerase, p1280 DNA, and primers Cb and 40F). To create p1293 (Table S1 of the Supporting Information), DNA fragment X, which was produced by ligating two *Sal*I-treated DNA fragments IX (synthesized by *Taq* polymerase, p1280 DNA, and primers Nf and 43B) and VIII (prepared by *Taq* polymerase, p1280 DNA, and primers Cb and 43F), was cloned to pET28a. Plasmid p1293 (Table S1 of the Supporting Information) was employed to make an rFKBP22 variant (designated rFKBP22I6) with a putative α3 helix of 44 amino acid residues. Strains SAU1289, SAU1290, SAU1291, SAU1292, and SAU1293 (Table S1 of the Supporting Information) were generated by transforming plasmids p1289, p1290, p1291, p1292, and p1293 to *E. coli* BL21(DE3), respectively.

Purification of Proteins. Proteins rFKBP22, rFKBP22D5, rFKBPP22D30, rFKBP22I3, and rFKBP22I6 were purified from *E. coli* strains SAU1289, SAU1290, SAU1291, SAU1292, and SAU1293, respectively, according to a previously described procedure.[12] Briefly, IPTG-induced cells in a buffer [20 mM Tris-HCl (pH 8.0), 500 mM NaCl, 20 mM imidazole, 5% glycerol, and 1 mM PMSF] were disrupted followed by the purification of the histidine-tagged protein from the crude extract by Ni-NTA column chromatography (Qiagen). The eluted protein was dialyzed against buffer B [20 mM Tris-HCl (pH 8.0), 300 mM NaCl, 1 mM EDTA, and 5% glycerol] or buffer C [100 mM phosphate buffer (pH 8.0), 300 mM NaCl, and 5% glycerol] for 12–16 h at 4 °C. SDS–13.5% PAGE analysis of each eluted protein fraction showed a single band (Figure S1 of the Supporting Information) that interacted with the anti-histidine antibody (data not shown). The molar concentrations of rFKBP22 and different rFKBP22 variants were determined using the molecular masses of their respective monomeric forms.

Activity of Proteins. To determine the PPIase activity of rFKBP22 and its variants (60 nM each), the RNase T1 (ribonuclease T1) refolding assay was performed as described previously.[12] To determine the k_{cat}/K_m (enzymatic activity) values, refolding data were analyzed with a standard equation.[2]

$$k_{cat}/K_m = (k_p - k_a)/[E] \quad (1)$$

where k_p and k_a indicate the first-order rate constants in the presence and absence of rFKBP22 or a derivative, respectively. The concentration of rFKBP22 or a derivative is denoted by [E]. The first-order rate constant ($k = k_p$ or k_a) was determined by nonlinear fitting of the refolding data to the following equation:

$$Y_t = (Y_0 - Y_\infty) \exp(-kt) + Y_\infty \quad (2)$$

where Y_t, Y_0, and Y_∞ represent the tryptophan fluorescence intensity values (λ_{em} = 323 nm, and λ_{ex} = 295 nm) at time t, at time zero, and at infinite time of RNase T1 refolding, respectively.

To determine the binding affinity of rapamycin for rFKBP22 or a derivative, rapamycin-mediated quenching of tryptophan fluorescence of the protein was studied as described previously.[12] Finally, the K_d (equilibrium dissociation constant) value of the rapamycin–protein interaction was calculated by nonlinear fitting of the quenched tryptophan fluorescence data

dx.doi.org/10.1021/bi300720g | *Biochemistry* 2012, 51, 7930–7939

to the following equation using GraphPad Prism (GraphPad Software Inc.).

$$Y = (B_{max}[X])/(K_d + [X]) \quad (3)$$

where Y denotes the extent of fluorescence quenched at any rapamycin concentration ([X]), which was determined according to a standard method.[12] B_{max} (i.e., maximal fluorescence quenched upon saturation of the protein with rapamycin) was determined from the double-reciprocal plot of $1/Y$ versus $1/[X]$.

Structural Characterization of Proteins. To study the structures of rFKBP22 and its different derivatives, far-UV circular dichroism (CD) spectra (200−260 nm) as well as near-UV CD spectra (250−310 nm) of these proteins were recorded by the standard methods.[20] To determine the extent of secondary structures, the far-UV CD spectra were analyzed with CDNN.[21] Protein concentrations for far- and near-UV CD experiments were 10 and 20 μM, respectively.

Protein rFKBP22 and its derivatives carry two tryptophan residues. To obtain a glimpse of the tryptophan environment of these macromolecules (10 μM each), their intrinsic tryptophan fluorescence spectra (λ_{em} = 300−400 nm, and λ_{ex} = 295 nm) were recorded essentially as described previously.[12,20,22] To determine the solvent accessibility of tryptophan residues of rFKBP22 and its derivatives, acrylamide quenching of tryptophan fluorescence of all these proteins was investigated as described previously.[12,23] To determine the Stern−Volmer constant (K_{sv}),[23] the quenched fluorescence data were analyzed with the following equation:

$$F_o/F = 1 + K_{sv}[Q] \quad (4)$$

where F_o, F, and [Q] represent the tryptophan fluorescence in the absence of acrylamide, the tryptophan fluorescence in the presence of acrylamide, and the acrylamide concentration, respectively.

Biochemical Methods. To determine the oligomeric status of rFKBP22 and its variants, a glutaraldehyde-mediated chemical cross-linking experiment with these macromolecules (10 μM each) was performed essentially as described previously.[12] To determine the molecular shape of rFKBP22 and its derivatives, analytical gel filtration chromatography was performed as described previously.[12]

Homology Modeling. The three-dimensional model structure of the *E. coli* FKBP22 monomer (harboring amino acid residues 9−205) was built with the I-TASSER server[24] using the crystal structure of *L. pneumophila* Mip (Protein Data Bank entry 1FD9)[13] as a template. The sequence of *L. pneumophila* Mip that carried amino acid residues 9- 47 was ∼40% homologous with that of *E. coli* FKBP22 harboring amino acid residues 8−47 (data not shown). As amino acid residues 9−47 are involved in the dimerization of *L. pneumophila* Mip monomers,[13] the homologous residues of two *E. coli* FKBP22 monomers were docked using the PatchDock server (http://bioinfo3d.cs.tau.ac.il/PatchDock). Molecular visualization of the resulting model structure was performed with Swiss-Pdb Viewer (http://ExPasy.org).

Unfolding and Refolding of Proteins. Protein rFKBP22 and its derivatives (10 μM each) in buffer B were treated with 0−7 M urea separately for 16−18 h at 4 °C followed by the recording of their CD as well as intrinsic tryptophan fluorescence spectra according to the methods described above. Aliquots of the freshly prepared stock solution of urea (10 M) were always used for treatment.

To probe the unfolding of rFKBP22 and its derivatives at the biochemical level, all these macromolecules (each 30 μg in 100 μL) were resolved separately through the transverse urea gradient gel (TUG) as described previously.[12,25] To test the reversibility of unfolding, urea-denatured proteins (such as rFKBP22 and its derivatives) were mixed with the gel loading dye (supplemented with 8 M urea) followed by their separation through similar TUG as stated above.

Analysis of Unfolding Curves. Considering that the urea-induced unfolding of rFKBP22 and its variants occurs by a two-state mechanism,[26] the fraction of unfolded protein molecules (f_u) was calculated using a standard equation (eq 5).

$$f_u = (X_n - X)/(X_n - X_u) \quad (5)$$

where X, X_n, and X_u denote the observed spectroscopic signal or mobility of the protein at any urea concentration, the spectroscopic signal or mobility of the protein in the completely folded state, and the spectroscopic signal or mobility of the protein in the completely unfolded state, respectively. The values of X_n and X_u were determined from the straight lines generated using the unfolding data at low and high urea concentrations (not shown).

C_m (urea concentration at the midpoint of the transition of the unfolding curve) values were determined by nonlinear fitting of the unfolding data to a standard equation (eq 6) using GraphPad Prism (GraphPad Software Inc.) as described previously.[12]

$$Y = \text{bottom} + (\text{top} - \text{bottom})/(1 + 10^{X - C_m}) \quad (6)$$

where X and Y indicate the concentration of urea and the fraction of unfolded protein molecules, respectively.

Statistical Analysis. All data presented here are means of at least three independent experiments with the standard deviation. Using AVERAGE, STDEV, and TTEST functions from Microsoft Excel, mean, standard deviation, and p values were determined, respectively. Two data were considered significant if the corresponding p value was <0.05.

RESULTS AND DISCUSSION

Purification of rFKBP22 and Its Mutant Derivatives. To map putative helix α3 of *E. coli* FKBP22 approximately, we have developed a model structure of this protein (Figure 1A) using an approach that is different from our earlier approach.[12] All modeling studies, however, indicated that the putative helix α3 in *E. coli* FKBP22 is unusually long and is composed of amino acid residues 55−92. To demonstrate whether the length of putative helix α3 of *E. coli* FKBP22 (Figure 1A) is critical for preserving its structure, function, and stability, we have designed, overexpressed, and purified a recombinant *E. coli* FKBP22 (rFKBP22) and four mutant derivatives (rFKBP22D5, rFKBP22D30, rFKBP22I3, and rFKBP22I6) to homogeneity (Figure S1 of the Supporting Information). All mutants harbor putative helix α3 of a distinct length (Figure 1B). To make helix α3 shorter or bigger, a separate in-frame mutation was introduced into the helix α3-forming regions of rFKBP22 (see Experimental Procedures for details). While the putative helix α3 regions of rFKBP22D5 and rFKBP22D30 lack 5 and 30 amino acid residues, respectively, those of rFKBP22I3 and rFKBP22I6 harbor an additional 3 and 6 amino acid residues, respectively. To avoid any possible helix break, inserted amino acid residues in the insertion mutants were selected from those that are involved in the formation of helix α3. Our

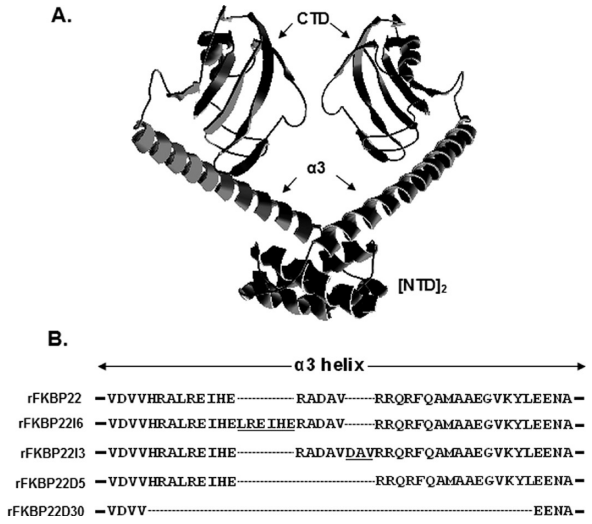

Figure 1. (A) Three-dimensional model structure of *E. coli* FKBP22. Development and visualization of the model structure were performed by the standard procedures as described in Experimental Procedures. The putative CTD (C-terminal domain), helix α3, and the NTD (N-terminal domain) in the homodimeric structure of FKBP22 are indicated. The NTD is involved in the dimerization of FKBP22 monomers. (B) Alignment of the amino acid sequences of the putative helix α3-forming regions in rFKBP22 and its mutant derivatives. Underlined amino acid residues were inserted into the helix α3-forming regions.

bioinformatic analysis indeed revealed that insertion or deletion did not cause any helix break but altered the length of helix α3 as expected (Figure 1B and data not shown).

Dimeric Status of Helix α3 Mutants. Insertion or deletion mutation in a protein may profoundly alter its different molecular properties (such as oligomeric status, secondary and tertiary structures, stability, function, etc.). To determine whether shortening or broadening the helix α3 has any effect on the dimeric status of FKBP22, we analyzed different concentrations of rFKBP22, rFKBP22D5, rFKBP22D30, rFKBP22I3, and rFKBP22I6 by gel filtration chromatography separately. Figure 2A shows that all proteins at 20 or 0.5 μM yielded a single peak with a distinct retention volume. Interestingly, there were ~1−4 mL increases in the elution volumes of the mutant proteins when their concentrations were decreased from 20 to 0.5 μM. In contrast, there was an only 0.25 mL increase in the elution volume of rFKBP22 under similar conditions. The retention volumes of rFKBP22, rFKBP22D30, and rFKBP22I6, however, were altered little at 2 μM (data not shown). Using the elution profiles of some standard proteins [such as conalbumin, ovalbumin, carbonic anhydrase, and ribonuclease A (data not shown)], the apparent molecular masses of all proteins were determined from their respective elution profiles. At 20 μM, the apparent molecular masses of rFKBP22, rFKBP22D5, rFKBP22D30, rFKBP22I3, and rFKBP22I6 were ~60.78, ~65.71, ~48.91, ~71.18, and ~80.95 kDa, respectively. Compared to the masses at 20 μM, the mass of rFKBP22 was ~2 kDa lower, whereas those of the mutant proteins were ~8−24 kDa lower at 0.5 μM, indicating that solution forms of the latter macromolecules might have been changed substantially at nanomolar concentration. Sequence analyses revealed that the molecular masses of rFKBP22, rFKBP22D5, rFKBP22D30, rFKBP22I3, and rFKBP22I6 monomers are

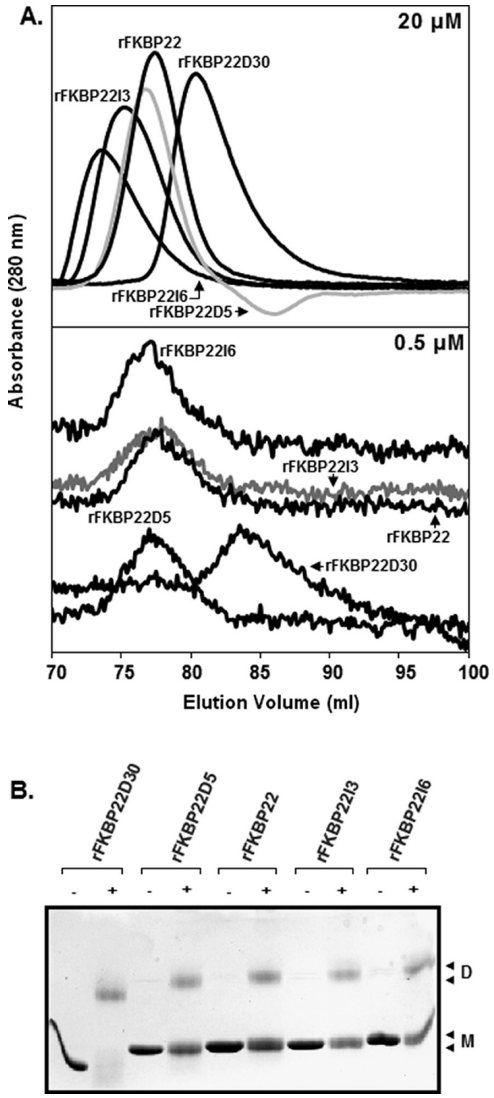

Figure 2. Determination of the molecular shape and oligomeric status of rFKBP22 and its derivatives. (A) Elution profiles of the indicated proteins by analytical gel filtration chromatography. All protein samples (20 or 0.5 μM) were injected onto a Superdex S-200 column. (B) Glutaraldehyde-treated (+) and untreated (−) proteins (all indicated) were analyzed by SDS−13.5% PAGE. The arrowhead denotes dimer-specific (D) and monomer-specific (M) protein bands.

~23.3, ~22.96, ~19.8, ~23.65, and ~24.14 kDa, respectively. Previously, *E. coli* FKBP22[1,12] and *Shewanella* FKBP22[16] were reported to exist as dimers in solution. As dilution did not drastically decrease the mass of rFKBP22, it might have been existed mostly as a dimer in solution at both micromolar and nanomolar concentrations. Because of the nonglobular structure, it was eluted a little earlier than expected. Like rFKBP22, a rFKBP22D30 molecule might be composed of two monomers that form a nonglobular conformation in solution at 20 μM. The elution volume of this deletion mutant at 0.5 μM (which is equivalent to the molecular mass of 35.21 kDa) indicates that it may be dissociated to a monomer partially at nanomolar concentrations. The single peak produced by 0.5 μM rFKBP22D30, therefore, may correspond to the average of its dimeric and monomeric forms, which are in rapid equilibrium with each other. Conversely, the peaks of three other helix α3 mutants correspond to trimers and dimers at 20

dx.doi.org/10.1021/bi300720g | *Biochemistry* 2012, 51, 7930−7939

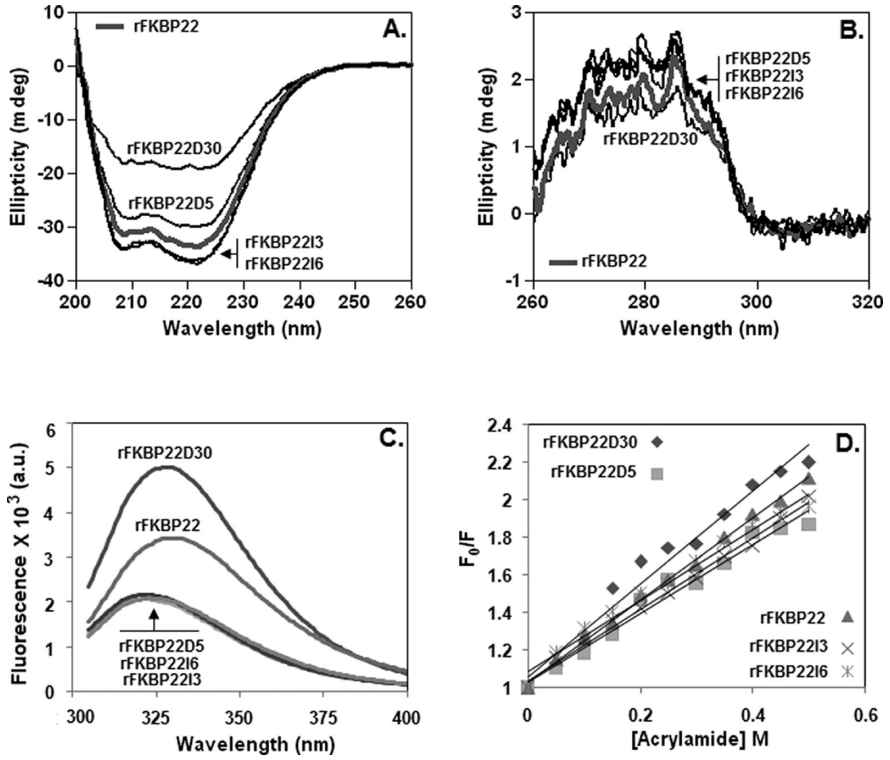

Figure 3. Biophysical characterization of rFKBP22 and its derivatives. Far-UV CD (A), near-UV CD (B), and intrinsic tryptophan (Trp) fluorescence (C) spectra of the indicated proteins were recorded at room temperature. (D) Stern–Volmer plots. Plots show the quenching of the Trp fluorescence of the indicated proteins in the presence of 0–0.5 M acrylamide solutions at room temperature.

and 0.5 μM, respectively. We rule out the formation of trimers, as our chemical cross-linking experiments revealed that all helix α3 mutants form dimers in solution only at higher concentrations (Figure 2B). The dimeric rFKBP22D5, rFKBP22I3, and rFKBP22I6 molecules possibly possess a more extended dimension than either rFKBP22 or rFKBP22D30, which in turn led to their early elution at 20 μM. At 0.5 μM, these latter mutants were possibly dissociated to the monomer partially like that of rFKBP22D30. Taken together, the data suggest that alteration of the length of helix α3 significantly affects both the dimension and dimerization ability of FKBP22.

Structures of the Helix α3 Mutants. To determine the effects of helix α3 mutations on the structure of *E. coli* FKBP22, we investigated the structures of rFKBP22 and its derivatives by various spectroscopic probes. The far-UV CD spectrum (200–260 nm) of each protein exhibited two peaks with large negative ellipticity at 208 and 222 nm (Figure 3A), indicating the presence of an α-helix in each protein. In comparison with the peaks in the spectrum of rFKBP22, the spectra of rFKBP22D5 and rFKBP22D30, however, carry reduced peaks, whereas those of rFKBP22I3 and rFKBP22I6 contain enlarged peaks, suggesting that these proteins are composed of variable amounts of α-helices. Analysis of the spectra by CDNN[21] indeed revealed that rFKBP22, rFKBP22D5, rFKBP22D30, rFKBP22I3, and rFKBP22I6 carry 25.7, 23.6, 18.2, 27.4, and 27.5% α-helix, respectively (Table S3 of the Supporting Information). The data together suggest that mutations in helix α3 affected the secondary structure of FKBP22 to some extent.

To assess the effects of helix α3 mutations on the tertiary structures of rFKBP22, near-UV CD spectra (260–320 nm) of all these proteins were recorded as described in Experimental Procedures. Each protein showed a flattened peak of positive ellipticity at ~270–290 nm (Figure 3B). None of the spectra of the mutant proteins, however, overlapped with that of rFKBP22. Interestingly, spectra of all mutant proteins except rFKBP22D30 overlapped partially. Taken together, insertion or deletion mutations in helix α3 possibly perturbed the tertiary structure of FKBP22 considerably. In addition, the tertiary structures of rFKBP22D5, rFKBP22I3, and rFKBP22I6 might share some homology.

Protein rFKBP22 and its mutant derivatives contain two Trp residues in their C-terminal domains. To understand the Trp environments in the proteins mentioned above, their intrinsic Trp fluorescence spectra were recorded after excitation at 295 nm. In comparison with the Trp fluorescence spectrum of rFKBP22, the Trp fluorescence spectrum of rFKBP22D30 yielded a higher fluorescence intensity, whereas those of other mutants produced reduced fluorescence intensities (Figure 3C). The latter mutant proteins produced nearly similar fluorescence intensities and exhibited emission maxima at ~323–324 nm. In contrast, the λ_{max} (wavelength of emission maxima) values observed for rFKBP22 and rFKBP22D30 were 327 and 328 nm, respectively. It is not clear why all mutant proteins (except rFKBP22D30) yielded the Trp fluorescence spectra with the blue-shifted emission maxima as well as less fluorescence intensity. The data, however, suggest that the Trp environments in all mutant proteins were altered significantly.

To precisely understand the effects of helix α3 mutations on the Trp environments of rFKBP22, we also studied the quenching of Trp fluorescence of these proteins in the presence of low concentrations of acrylamide. The Stern–Volmer plots,[12] derived from the acrylamide quenching data of the Trp fluorescence of the five recombinant proteins, were found to be linear (Figure 3D). The K_{sv} (Stern–Volmer constants)

dx.doi.org/10.1021/bi300720g | *Biochemistry* 2012, 51, 7930–7939

values, determined from the slopes of the Stern−Volmer plots, appeared to vary from 1.85 ± 0.04 to 2.43 ± 0.04 M^{-1} (Table 1). Compared to the K_{sv} value of rFKBP22, the K_{sv} value of

Table 1. k_{cat}/K_m, K_{sv}, and K_d Values

protein	K_{sv} $(M^{-1})^a$	k_{cat}/K_m $(\mu M^{-1}\ s^{-1})^b$	K_d $(\mu M)^c$
rFKBP22	2.12 ± 0.07	0.932 ± 0.025	6.65 ± 0.26
rFKBP22D5	1.86 ± 0.05	0.029 ± 0.002	7.91 ± 1.10
rFKBP22D30	2.43 ± 0.04	0.004 ± 0.0001	6.64 ± 0.14
rFKBP22I3	1.85 ± 0.06	0.131 ± 0.001	8.82 ± 1.53
rFKBP22I6	1.85 ± 0.04	0.029 ± 0.001	7.39 ± 0.68

[a]Stern−Volmer constants (K_{sv}) were determined from the slopes of the plots presented in Figure 3D. [b]k_{cat}/K_m values were determined from Figure 4A. [c]K_d values were determined from Figure 4B.

rFKBP22D30 is significantly higher ($p < 0.027$), whereas those of other mutants are considerably smaller (all $p < 0.05$). The data indicate that deletion of 30 amino acid residues from the helix α3-forming region partially enhanced the accessibility of the Trp residues in the CTD. In contrast, other mutations reduced the accessibility of the Trp residues to some extent.

Refolding and Drug Binding Abilities of Helix α3 Mutants. To determine whether the alteration of the length of helix α3 has any role in the PPIase (peptidyl-prolyl *cis*−*trans* isomerase) activity of FKBP22, we performed the RNase T1 refolding assay in the presence of rFKBP22 and its derivatives separately. Figure 4A shows that rFKBP22D30 possesses almost no PPIase activity, whereas catalytic activities of other mutant proteins are lower than that of rFKBP22. The k_{cat}/K_m (catalytic activity) values for rFKBP22, rFKBP22D30, rFKBP22D5, rFKBP22I3, and rFKBP22I6 were determined (from Figure 4A) and found to be 0.932 ± 0.025, 0.004 ± 0.0001, 0.029 ± 0.002, 0.131 ± 0.001, and 0.029 ± 0.001 $\mu M^{-1}\ s^{-1}$, respectively (Table 1). As the k_{cat}/K_m values of the mutant proteins were estimated to be ∼7−233-fold lower, we suggest that deletion or insertion mutation in the helix α3-forming region severely affects the catalytic efficiency of FKBP22.

Our investigations indicated that mutations in the helix α3 region of FKBP22 considerably affected the structures of its two domains (see above). To determine whether the altered conformations of the C-terminal domains of the mutant FKBP22 proteins have changed their drug binding affinities, we performed the rapamycin-mediated Trp fluorescence quenching assay as described in Experimental Procedures. Figure 4B shows the quenching of the Trp fluorescence of rFKBP22 and its mutant derivatives in the presence of 0−40 μM rapamycin. The K_d values for the interactions between rapamycin and all proteins were determined (from Figure 4B) and found to vary from 6.64 ± 0.14 to 8.82 ± 1.53 μM (Table 1). The data indicate that mutations in helix α3 of FKBP22 did not notably alter its drug binding affinity.

Effects of Urea on the Structures of rFKBP22 and Its Derivatives. Exposure of a protein to any denaturant usually alters its structure, function, and stability. To see whether urea (a neutral denaturant) affects the secondary structures of rFKBP22 and its derivatives, we recorded the far-UV CD spectra of all these proteins in the presence of 0−7 M urea (Figure S2A−E of the Supporting Information). The magnitudes of the peaks of the far-UV spectra of rFKBP22, rFKBP22D5, rFKBP22I3, and rFKBP22I6 at 222 nm were gradually decreased when urea concentrations were increased from ∼3 to 5 M. In contrast, the peaks of rFKBP22D30-specific spectra at 222 nm were reduced progressively at ∼2−5 M urea. The peaks of none of the proteins at 222 nm were diminished further at urea concentrations of >5 M. The data together indicate that the α-helical content of rFKBP22D30 began decreasing at urea concentrations greater than ∼2 M, whereas those of the rest of the proteins started decreasing at urea concentrations of >3 M. Because of complete denaturation, the α-helices in all proteins were lost at urea concentrations of >5 M. Collectively, the helix content of rFKBP22D30 appeared to be affected more severely than those of other proteins in the presence of urea.

To determine the effect of urea on the Trp environment of rFKBP22 and its derivatives, intrinsic Trp fluorescence spectra of all these proteins (pre-equilibrated with 0−7 M urea) were recorded at room temperature (see Experimental Procedures for details). The resulting spectra show that Trp fluorescence intensities and λ_{max} values of all proteins were changed drastically at distinct urea concentrations (Figure S2F−J of the Supporting Information). While the fluorescence intensity and λ_{max} values of rFKBP22D30 were increased gradually when the urea concentration was increased from ∼1.5 to 4.25 M, those of other proteins, including rFKBP22, started increasing at urea concentrations of ∼2.5 M and higher. The fluorescence intensities of rFKBP22D30 tended to saturate at ∼4.25−7 M with λ_{max} values of 348−349 nm. Other proteins exhibited such properties at urea concentrations of ∼4.75−7 M. The results together suggest that unfolding of rFKBP22D30 was started and completed at urea concentrations of ∼1.5 and ∼4.25 M, respectively. rFKBP22D30 remained as a completely folded

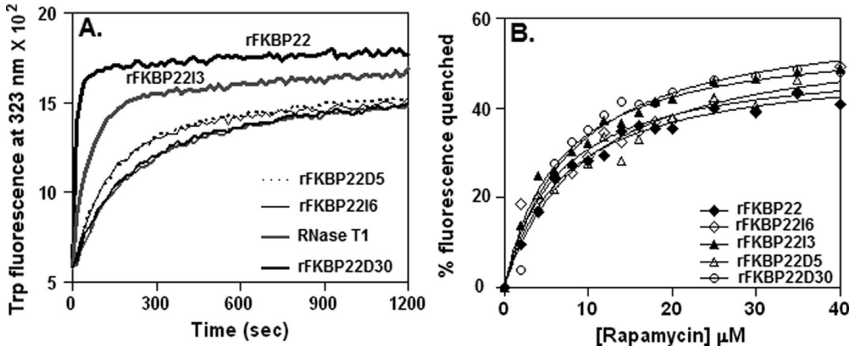

Figure 4. Functional characterization of rFKBP22 and its derivatives. (A) RNase T1 refolding assay. Refolding of RNase T1 was performed in the presence and absence of the indicated proteins at 10 °C. (B) Rapamycin binding assay. The plot shows the quenching of Trp fluorescence intensity of all five proteins (5 μM each) in the presence of 0−40 μM rapamycin.

dx.doi.org/10.1021/bi300720g | *Biochemistry* 2012, 51, 7930−7939

state at ~0−1.5 M urea but existed as different mixtures of folded and unfolded forms at ~1.5−4.25 M urea. In contrast, initiation and termination of the unfolding of other mutants and rFKBP22 occurred comparatively at higher urea concentrations.

Mechanism of Urea-Induced Unfolding. To understand the mechanism of urea-induced unfolding of rFKBP22 and its derivatives, the fraction of unfolded protein molecules, determined from the far-UV CD and Trp fluorescence intensity data (Figure S2 of the Supporting Information) using eq 5, were plotted versus the corresponding urea concentrations. The resulting unfolding curves are all sigmoidal in nature with one transition in the presence of urea (Figure 5A). Of the monophasic curves, rFKBP22- and rFKBP22D5-specific curves appeared to be completely superimposable, whereas those of rFKBP22I3, rFKBP22I6, and rFKBP22D30 did not overlap, particularly in the transition regions. All the unfolding curves though were found to fit nicely to a two-state equation (eq 6), and unfolding of the latter three proteins may not follow the two-state mechanism like those of the former two proteins in the presence of urea. The noncoincidence of the rFKBP22I3-, rFKBP22I6-, and rFKBP22D30-specific curves may arise because of the initiation of unfolding of their domains at different urea concentrations. Currently, the urea concentrations needed to start the unfolding of the domains of the three helix α3 mutants mentioned above are not known clearly. Previously, urea-induced unfolding of a recombinant *E. coli* FKBP22 was reported to occur by a two-state mechanism, though unfolding of its domains was initiated at dissimilar urea concentrations.[12] Urea-induced unfolding of a recombinant human FKBP12 was also suggested to follow the two-state mechanism, though there was noncoincidence of the associated unfolding curves derived from the CD and Trp fluorescence experiments.[27]

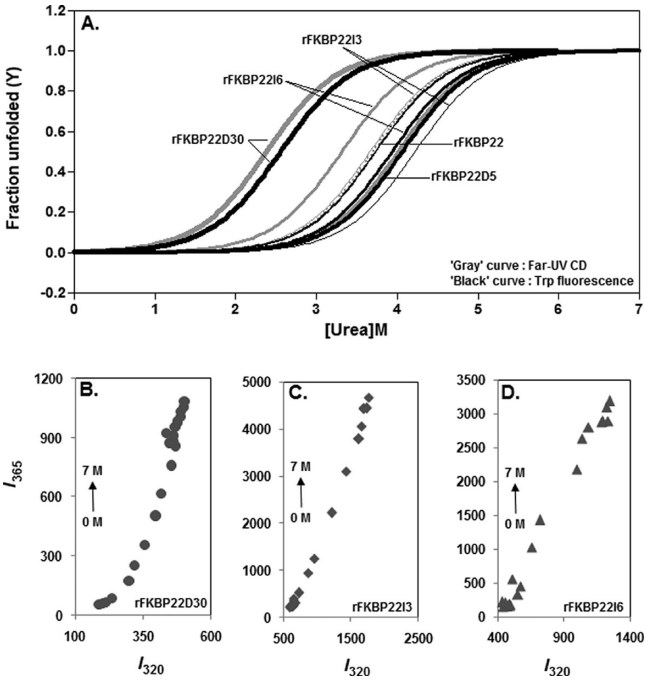

Figure 5. Mechanism of urea-induced unfolding of rFKBP22 and its helix α3 mutants. (A) Fraction of unfolded protein (Y) in the presence and absence of urea. Y values were calculated from the far-UV circular dichroism (CD) and intrinsic Trp fluorescence data (Figure S2 of the Supporting Information) of the indicated proteins and plotted vs urea concentration by the standard procedures as described previously.[12] (B−D) Phase diagrams showing the unfolding of rFKBP22D30 (B), rFKBP22I3 (C), and rFKBP22I6 (D) in the presence of 0−7 M urea. I_{320} and I_{365} denote the fluorescence intensities of a protein at 320 and 365 nm, respectively.

The phase diagram, a qualitative tool, has long been employed to identify the hidden unfolding−refolding intermediates of proteins.[28−30] Such a tool appeared to be very useful particularly when there is the lack of coincidence of the unfolding curves of proteins. To verify whether rFKBP22I3, rFKBP22I6, and rFKBP22D30 unfold with the formation of one or more intermediates, we constructed phase diagrams for all these proteins by plotting their Trp fluorescence intensity values at 320 nm versus the respective Trp fluorescence intensity values at 365 nm. All three proteins in the diagrams yielded nearly linear plots at 0−7 M urea (Figure 5B−D). Phase diagrams developed for rFKBP22 and rFKBP22D5 also produced linear plots (data not shown). The data together indicate that rFKBP22 and its derivatives do not form any intermediate during their unfolding in the presence of urea.

The C_m (urea concentration at the midpoint of the unfolding transition) values were determined from the fitted unfolding data (Figure 5A) and are listed in Table 2. The C_m value of rFKBP22D30 appeared to be significantly lower than those of other mutants and rFKBP22 (all p values of <0.02), indicating that rFKBP22D30 is the least stable of the five proteins. In contrast, the C_m value of rFKBP22D5 was found to be considerably higher than that of the control protein (p = 0.015). The C_m values of rest of the mutant proteins were also higher when these values were determined from the respective Trp fluorescence data. As Trp fluorescence spectroscopy is more sensitive than CD spectroscopy, we suggest that rFKBP22I3 and rFKBP22I6 are relatively more stable than rFKBP22. Interestingly, the C_m values of rFKBP22D5 and rFKBP22I6 that seemed to be nearly similar were notably lower than that of rFKBP22I3 (all p values of <0.05). The data together indicate that rFKBP22I3 is the most stable of the five proteins studied here.

To confirm the unfolding mechanism of rFKBP22 and its variants, all these proteins were analyzed by transverse urea gradient gel electrophoresis (TUGE) as described previously.[12,25] Migration of the helix α3 mutants and rFKBP22

Table 2. C_m Values from Different Unfolding Assays[a]

	C_m				
assay type	rFKBP22D30	rFKBP22D5	rFKBP22	rFKBP22I3	rFKBP22I6
far-UV CD	2.38 ± 0.06	4.01 ± 0.01	3.71 ± 0.02	3.67 ± 0.04	3.32 ± 0.04
Trp fluorescence	2.56 ± 0.03	4.06 ± 0.02	3.73 ± 0.04	4.22 ± 0.04	3.94 ± 0.05
TUGE	2.92 ± 0.08	4.12 ± 0.06	3.80 ± 0.04	4.47 ± 0.01	4.50 ± 0.06

[a] C_m values were determined by fitting the equilibrium unfolding data (presented in Figures 5A and 6A,B) to eq 6.

dx.doi.org/10.1021/bi300720g | *Biochemistry* 2012, 51, 7930−7939

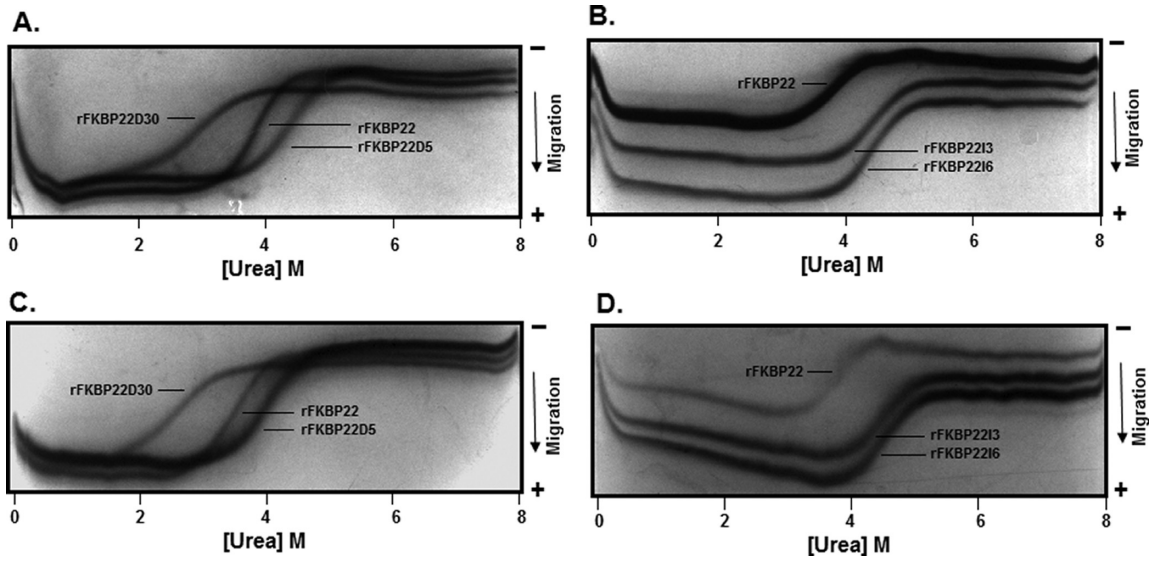

Figure 6. Mobility of native (A and B) and unfolded (C and D) rFKBP22 and its derivatives across the transverse urea gradient polyacrylamide gel.

across the 0 to 8 M urea gradient yielded the bands having the shapes of a monophasic curve (Figure 6A,B). The native, transition, and unfolded states of the proteins, as exhibited by the monophasic curvelike bands, however, were not obtained exactly at identical urea concentrations. While the transition region of rFKBP22D30 appeared at ∼2−3.75 M urea, those of rFKBP22, rFKBP22D5, rFKBP22I3, and rFKBP22I6 were noticed at ∼3−4, ∼3.75−5, ∼3.85−5, and ∼3.9−5.25 M urea, respectively. Because of the gradual increase in the levels of the denatured forms, mobilities of the proteins were decreased steadily upon enhancement of urea concentrations at the transition region. At urea concentrations below those involved in the formation of the transition region, all proteins remained in the folded state and migrated roughly as linear bands. All proteins also migrated as linear bands at urea concentrations higher than those involved in the conformational transition from folded to unfolded states. Proteins under the latter conditions, however, remained in the completely unfolded state and moved slowly in comparison with those of the corresponding folded molecules. Such migration patterns confirmed the spectroscopic data (Figure 6A) and clearly showed that urea-induced unfolding of all five proteins follows the two-state mechanism with the formation of the unfolded form directly from the native form. The C_m values for rFKBP22, rFKBP22D5, rFKBP22D30, rFKBP22I3, and rFKBP22I6 were determined from the respective TUGE pictures and are listed in Table 2. The results again indicate that rFKBP22D30 is the least stable protein as its C_m value is significantly lower than those of other mutants and rFKBP22 (all p values of <0.05). In addition, rFKBP22D5, rKBP22I3, and rFKBP22I6 were found to be more stable than rFKBP22. For unknown reasons, both the insertion mutants exhibited nearly equal stability in the study with TUGE. rFKBP22D5 was also less stable than rFKBP22I6. The suggestions made from Trp fluorescence spectroscopy (see above), however, might be trustworthy, as it is more sensitive than CD spectroscopy or TUGE.

The TUGE images (Figure 6A,B) show that the band patterns of rFKBP22 and its mutants are very sharp, particularly in the transition regions. It indicates that the native and unfolded forms of each protein may be in rapid equilibrium with absolutely no accumulation of intermediates.[25] To prove the hypothesis, unfolded rFKBP22 and its derivatives were also similarly analyzed by TUGE (see above). If the folded and unfolded proteins are really in rapid equilibrium, unfolded proteins will also yield sigmoidal band patterns with sharp transition regions.[25] The TUGE pictures in panels C and D of Figure 6 indeed reveal that band patterns of unfolded rFKBP22 and its derivatives are quite similar to those produced by the corresponding folded proteins. Even the C_m values of the unfolded proteins (determined from panels C and D of Figure 6) matched those of the corresponding folded proteins (data not shown). The data together indicate that urea-induced unfolding of rFKBP22 and its variants is reversible in nature.

Our investigations revealed that the dimerization, structure, stability, and protein substrate refolding ability were affected severely, whereas the drug binding ability of *E. coli* FKBP22 was affected little by the deletion and insertion mutations in its putative helix α3 region. The conformation of the CTD of FKBP22 was distorted considerably upon deletion of amino acid residues from helix α3 or insertion of amino acid residues into helix α3 (Figure 3). Despite the modification, the drug binding activity of the C-terminal domain remained unaltered, indicating that reducing or increasing the length of helix α3 did not cause any damage to the region that performs the function mentioned above.

In addition to the putative V-shaped structure,[12] the length of helix α3 of FKBP22 appeared to be essential for its PPIase activity with RNase T1 (Figure 4A). As the C-terminal domains of *E. coli* FKBP22 and the related proteins were thought to carry the catalytic site for PPIase,[12,16,31,32] the way in which helix α3 contributes to enzyme activity is not exactly clear. Previously, the NTD of SIB1 FKBP22 was shown to be crucial for its PPIase activity with RNase T1.[33] It was suggested that the NTD is involved in the binding of the protein substrate. Possibly, helix α3 too somehow holds RNase T1 that in turn assists the CTD in performing its catalytic function. With an increase or decrease in the length of helix α3, the CTD possibly did not properly connect with RNase T1. Alternatively, an altered helix α3 may not bind RNase T1 tightly.

The unfolding study revealed that the length of helix α3 contributes significantly to the stability of *E. coli* FKBP22

dx.doi.org/10.1021/bi300720g | *Biochemistry* 2012, 51, 7930−7939

(Figure 5A and Table 2). While deletion of 30 amino acid residues from helix α3 reduced the stability, deletion of 5 amino acid residues or insertion of 3−6 amino acid residues considerably enhanced the stability of FKBP22. The results were quite unexpected as the side chains of the amino acid residues in helix α3 are not involved in any bonding or interaction with the residues in the domains.[13] A large number of salt bridges in helix α3 of *Legionella* Mip[13] were thought to be involved in its stability. Most possibly, the substantial loss of the salt bridges from helix α3 contributed to the decreased stability of rFKBP22D30. It is not clear what determinants have made other mutants more stable than rFKBP22.

CONCLUSIONS

E. coli FKBP22 and the related proteins carry a long α-helix (designated α3) between their two domains. Using two helix α3 deletion mutants and two helix α3 insertion mutants of *E. coli* FKBP22, we have demonstrated that the length of helix α3 is indispensable for preserving the molecular dimension, dimeric status, secondary structure, tertiary structure, and protein substrate refolding ability of this protein. Shortening or extending the length of helix α3, however, did not considerably affect its drug binding affinity. Additional investigation revealed that deletion of 30 amino acid residues from the helix α3-forming region severely affected its stability, whereas insertion of 3−6 amino acid residues or deletion of 5 amino acid residues from the same region notably enhanced its stability.

ASSOCIATED CONTENT

Supporting Information

Purification of rFKBP22 and its derivatives (Figure S1), urea-induced equilibrium unfolding of rFKBP22 and its variants (Figure S2), bacterial strains and plasmids used in this study (Table S1), oligonucleotides used in this study (Table S2), and secondary structural elements in rFKBP22 and its derivatives (Table S3). This material is available free of charge via the Internet at http://pubs.acs.org.

AUTHOR INFORMATION

Corresponding Author

*E-mail: subratasau@gmail.com or subratasau@yahoo.co.in. Telephone: 91-33-2355-9416. Fax: 91-33-2355-3886.

Funding

The work was supported by a grant from CSIR, Government of India [37(1427)/04/EMR-II], to S.S. B.J. received a Senior Research Fellowship from the Department of Atomic Energy (Government of India).

Notes

The authors declare no competing financial interest.

ACKNOWLEDGMENTS

We thank Dr. G. Chakrabarti (University of Calcutta, Kolkata, India) for critically reading and correcting the manuscript. We also thank Mr. A. Banerjee, Mr. A. Poddar, Mr. J. Guin, and Mr. M. Das for their excellent technical support.

ABBREVIATIONS

FKBP22, PPIase (peptidyl-prolyl *cis*−*trans* isomerase) from *E. coli*; rFKBP22, C-terminally histidine-tagged FKBP22; rFKBP22D5, rFKBP22 derivative whose five helix α3-forming amino acid residues were deleted; rFKBP22D30, rFKBP22 derivative whose 30 helix α3-forming amino acid residues were deleted; rFKBP22I3, rFKBP22 derivative that carries three additional amino acid residues within its helix α3-forming region; rFKBP22I6, rFKBP22 derivative that carries additional six additional amino acid residues within its helix α3-forming region; TUGE, transverse urea gradient gel electrophoresis.

REFERENCES

(1) Rahfeld, J. U., Rucknagel, K. P., Stoller, G., Horne, S. M., Schierhorn, A., Young, K. D., and Fischer, G. (1996) Isolation and amino acid sequence of a new 22-kDa FKBP-like peptidyl-prolyl *cis/trans*-isomerase of *Escherichia coli*. Similarity to Mip-like proteins of pathogenic bacteria. *J. Biol. Chem. 271*, 22130−22138.

(2) Göthel, S. F., and Marahiel, M. A. (1999) Peptidyl-prolyl *cis-trans* isomerases, a superfamily of ubiquitous folding catalysts. *Cell. Mol. Life Sci. 55*, 423−436.

(3) Engleberg, N. C., Carter, C., Weber, D. R., Cianciotto, N. P., and Eisenstein, B. I. (1989) DNA sequence of *mip*, a *Legionella pneumophila* gene associated with macrophage infectivity. *Infect. Immun. 57*, 1263−1270.

(4) Lundemose, A. G., Kay, J. E., and Pearce, J. H. (1993) *Chlamydia trachomatis* Mip-like protein has peptidyl-prolyl *cis/trans* isomerase activity that is inhibited by FK506 and rapamycin and is implicated in initiation of chlamydial infection. *Mol. Microbiol. 7*, 777−783.

(5) Horne, S. M., and Young, K. D. (1995) *Escherichia coli* and other species of the Enterobacteriaceae encode a protein similar to the family of Mip-like FK506-binding proteins. *Arch. Microbiol. 163*, 357−365.

(6) Ramm, K., and Pluckthun, A. (2000) The periplasmic *Escherichia coli* peptidylprolyl *cis,trans*-isomerase FkpA. II. Isomerase-independent chaperone activity *in vitro*. *J. Biol. Chem. 275*, 17106−17113.

(7) Moro, A., Ruiz-Cabello, F., Fernandez-Cano, A., Stock, R. P., and Gonzalez, A. (1995) Secretion by *Trypanosoma cruzi* of a peptidyl-prolyl *cis-trans* isomerase involved in cell infection. *EMBO J. 14*, 2483−2490.

(8) Leuzzi, R., Serino, L., Scarselli, M., Savino, S., Fontana, M. R., Monaci, E., Taddei, A., Fischer, G., Rappuoli, R., and Pizza, M. (2005) Ng-MIP, a surface-exposed lipoprotein of *Neisseria gonorrhoeae*, has a peptidyl-prolyl *cis/trans* isomerase (PPIase) activity and is involved in persistence in macrophages. *Mol. Microbiol. 58*, 669−681.

(9) Zang, N., Tang, D. J., Wei, M. L., He, Y. Q., Chen, B., Feng, J. X., Xu, J., Gan, Y. Q., Jiang, B. L., and Tang, J. L. (2007) Requirement of a *mip*-like gene for virulence in the phytopathogenic bacterium *Xanthomonas campestris pv*. campestris. *Mol. Plant-Microbe Interact. 20*, 21−30.

(10) Horne, S. M., Kottom, T. J., Nolan, L. K., and Young, K. D. (1997) Decreased intracellular survival of an *fkpA* mutant of *Salmonella typhimurium* Copenhagen. *Infect. Immun. 65*, 806−810.

(11) Suzuki, Y., Haruki, M., Takano, K., Morikawa, M., and Kanaya, S. (2004) Possible involvement of an FKBP family member protein from a psychrotrophic bacterium *Shewanella* sp. SIB1 in cold-adaptation. *Eur. J. Biochem. 271*, 1372−1381.

(12) Jana, B., Bandhu, A., Mondal, R., Biswas, A., Sau, K., and Sau, S. (2012) Domain structure and denaturation of a dimeric Mip-like peptidyl-prolyl *cis-trans* isomerase from *Escherichia coli*. *Biochemistry 51*, 1223−1237.

(13) Riboldi-Tunnicliffe, A., Konig, B., Jessen, S., Weiss, M. S., Rahfeld, J., Hacker, J., Fischer, G., and Hilgenfeld, R. (2001) Crystal structure of Mip, a prolylisomerase from *Legionella pneumophila*. *Nat. Struct. Biol. 8*, 779−783.

(14) Saul, F. A., Arie, J. P., Vulliez-le Normand, B., Kahn, R., Betton, J. M., and Bentley, G. A. (2004) Structural and functional studies of FkpA from *Escherichia coli*, a *cis/trans* peptidyl-prolyl isomerase with chaperone activity. *J. Mol. Biol. 335*, 595−608.

(15) Budiman, C., Bando, K., Angkawidjaja, C., Koga, Y., Takano, K., and Kanaya, S. (2009) Engineering of monomeric FK506-binding protein 22 with peptidyl prolyl *cis-trans* isomerase. Importance of a V-shaped dimeric structure for binding to protein substrate. *FEBS J. 276*, 4091−4101.

(16) Suzuki, Y., Takano, K., and Kanaya, S. (2005) Stabilities and activities of the N- and C-domains of FKBP22 from a psychrotrophic bacterium overproduced in *Escherichia coli*. *FEBS J. 272*, 632−642.
(17) Sambrook, J., and Russell, D. W. (2001) *Molecular cloning: A laboratory manual*, 3rd ed., Cold Spring Harbor Laboratory Press, Plainview, NY.
(18) Ausubel, F. M. (1987) *Current protocols in molecular biology*, Greene Publishing Associates and Wiley-Interscience, New York.
(19) Bradford, M. M. (1976) A rapid and sensitive method for the quantitation of microgram quantities of protein utilizing the principle of protein-dye binding. *Anal. Biochem. 72*, 248−254.
(20) Creighton, T. E. (1997) *Protein Structure: A Practical Approach*, 2nd ed., IRL Press at Oxford University Press, New York.
(21) Bohm, G., Muhr, R., and Jaenicke, R. (1992) Quantitative analysis of protein far UV circular dichroism spectra by neural networks. *Protein Eng. 5*, 191−195.
(22) Lakowicz, J. R. (1999) *Principles of fluorescence spectroscopy*, 2nd ed., Kluwer Academic/Plenum, New York.
(23) Eftink, M. R., and Ghiron, C. A. (1981) Fluorescence quenching studies with proteins. *Anal. Biochem. 114*, 199−227.
(24) Zhang, Y. (2008) I-TASSER server for protein 3D structure prediction. *BMC Bioinf. 9*, 40.
(25) Goldenberg, D. P., and Creighton, T. E. (1984) Gel electrophoresis in studies of protein conformation and folding. *Anal. Biochem. 138*, 1−18.
(26) Pace, C. N., and Shaw, K. L. (2000) Linear extrapolation method of analyzing solvent denaturation curves. *Proteins 4* (Suppl.), 1−7.
(27) Egan, D. A., Logan, T. M., Liang, H., Matayoshi, E., Fesik, S. W., and Holzman, T. F. (1993) Equilibrium denaturation of recombinant human FK binding protein in urea. *Biochemistry 32*, 1920−1927.
(28) Kuznetsova, I. M., Turoverov, K. K., and Uversky, V. N. (2004) Use of the phase diagram method to analyze the protein unfolding-refolding reactions: Fishing out the "invisible" intermediates. *J. Proteome Res. 3*, 485−494.
(29) Cellini, B., Bertoldi, M., Montioli, R., Laurents, D. V., Paiardini, A., and Voltattorni, C. B. (2006) Dimerization and folding processes of *Treponema denticola* cystalysin: The role of pyridoxal 5′-phosphate. *Biochemistry 45*, 14140−14154.
(30) Ludwig, H. C., Pardo, F. N., Asenjo, J. L., Maureira, M. A., Yañez, A. J., and Slebe, J. C. (2007) Unraveling multistate unfolding of pig kidney fructose-1,6-bisphosphatase using single tryptophan mutants. *FEBS J. 274*, 5337−5349.
(31) Köhler, R., Fanghanel, J., Konig, B., Luneberg, E., Frosch, M., Rahfeld, J. U., Hilgenfeld, R., Fischer, G., Hacker, J., and Steinert, M. (2003) Biochemical and functional analyses of the Mip protein: Influence of the N-terminal half and of peptidylprolyl isomerase activity on the virulence of *Legionella pneumophila*. *Infect. Immun. 71*, 4389−4397.
(32) Ceymann, A., Horstmann, M., Ehses, P., Schweimer, K., Paschke, A., Michael Steinert, M., and Faber, C. (2008) Solution structure of the *Legionella pneumophila* Mip-rapamycin complex. *BMC Struct. Biol. 8*, 17.
(33) Suzuki, Y., Win, O. Y., Koga, Y., Takano, K., and Kanaya, S. (2005) Binding analysis of a psychrotrophic FKBP22 to a folding intermediate of protein using surface plasmon resonance. *FEBS Lett. 579*, 5781−5784.